Journal of Cultural Heritage 60 (2023) 63–71

Contents lists available at ScienceDirect

Journal of Cultural Heritage

journal homepage: www.elsevier.com/locate/culher

Short communication

Archaeometric research on decorated bricks of Tol-e Ajori monumental gate (6th century BC), Fars, Iran: New insight into the glazes

Maria Letizia Amadori[a,*], Emad Matin[b], Gianluca Poldi[c], Valeria Mengacci[a], Jgor Arduini[a], Pierfrancesco Callieri[d], Alireza Askari Chaverdi[e], Parviz Holakooei[f]

[a] Department of Pure and Applied Sciences, University of Urbino, Piazza Rinascimento 6, 61029 Urbino, Italy
[b] ISMEO, Corso Vittorio Emanuele II 244, Palazzo Baleani, 00186 Rome, Italy
[c] Department of Letters, Philosophy and Communication, University of Bergamo, Via Pignolo 76, 24121 Bergamo, Italy
[d] Department of Cultural Heritage, University of Bologna, via degli Ariani 1, 48121 Ravenna, Italy
[e] Department of History and Archaeology, College of Literature and Humanities, Shiraz University (CISSC), Eram Square, 71944 Shiraz, Iran
[f] Department of Conservation and Restoration of Historic Properties, Art University of Isfahan, Hakim-Nezami St., P.O. Box 1744, Isfahan, Iran

ARTICLE INFO

Article history:
Received 6 July 2022
Accepted 17 January 2023
Available online 16 February 2023

Keywords:
Achaemenid
Tol-e Ajori monumental gate
Glazed bricks
Brizziite
Antimonates
Co-Cu

ABSTRACT

The archaeological excavations ongoing since 2011 at Tol-e Ajori – located 3.5 km NW of the Persepolis Terrace – discovered an Achaemenid monumental gate dating back to the second half of the 6th century BC. Thousands of glazed clay bricks, flat or in relief with decorative and figurative motifs, which are very similar to the bricks of Babylon's Ishtar Gate, were unearthed from Tol-e Ajori. As the glazed surfaces of the bricks were seriously degraded, due to the long period of burial, a set of non-invasive investigations was first carried out to identify the original hues, also in situ, using digital microscopy, portable energy dispersive X-ray fluorescence (ED-XRF) and visible reflectance spectrometry (Vis-RS). Minute samples were also investigated by micro-X-ray fluorescence (μ-XRF), polarised light microscopy (PLM), scanning electron microscopy with energy-dispersive X-ray spectroscopy (ESEM-EDS), and micro-Raman spectroscopy.

The occurrence of brizziite (sodium antimonate, $NaSbO_3$) and calcium antimonate ($CaSb_2O_6$) as white opacifiers embedded in the lime-alkali glaze was evinced. Lead antimonate was also shown to be a yellow opacifier while cobalt and copper occur as colouring agents in the blue glazes. The greenish hues were obtained by mixing Cu^{2+} with the yellow opacifier. These results are coherent with the general knowledge available on the Iron Age glaze production in the ancient Near East. Moreover, the iconographical and archaeological features suggested close ties between the glazed bricks from Tol-e Ajori monumental gate and the Ishtar Gate. We also considered the similarities and differences between glaze technology evidenced in Tol-e Ajori and important archaeological sites in Iran and Iraq. In addition, the source of Co in the glazes from Tol-e Ajori bricks and other Achaemenid glazed bricks from Susa and the Persepolis Terrace is discussed.

1. Introduction

The excavations ongoing from 2011 by the "Iranian-Italian Joint Archaeological Mission in Fars" in the Persepolis area (Marvdasht plain) (Fig. S1a), unearthed an Achaemenid monumental gate in the site of Tol-e Ajori, located 3.5 km to the west of the Persepolis Terrace and dated to the second half of the 6th century BC [1–3]. The Tol-e Ajori building (Fig. S1b) measures 39.07 m (NW-SE) × 29.05 m (NE-SW). The glazed bricks were part of the preserved sections of the building's wall (in situ) and the thousands of glazed fragments found in the accumulation and collapse layers give evidence of an original rich glazed relief and flat decoration (Fig. 1a,b). The glazed bricks were marked on the upper faces with a series of simple signs – called fitters' marks – to show the bricklayers the right position of each brick [4–6]. Similar fitters' marks have been found on other ancient Near East glazed bricks [7,8].

Data from literature related to Babylonian decorated bricks highlighted an exceptional similarity with the same materials from pre-Achaemenid Babylon, especially the glazed clay bricks decorating the last phase of the Neo-Babylonian Ishtar Gate (6th century BC). This similarity is so strong to stress that almost all of the fragments of bricks of Tol-e Ajori belonged to the same motifs visible on the Babylonian bricks [4–6]. In particular, the glazed relief

* Corresponding author.
E-mail address: maria.amadori@uniurb.it (M.L. Amadori).

https://doi.org/10.1016/j.culher.2023.01.005
1296-2074/

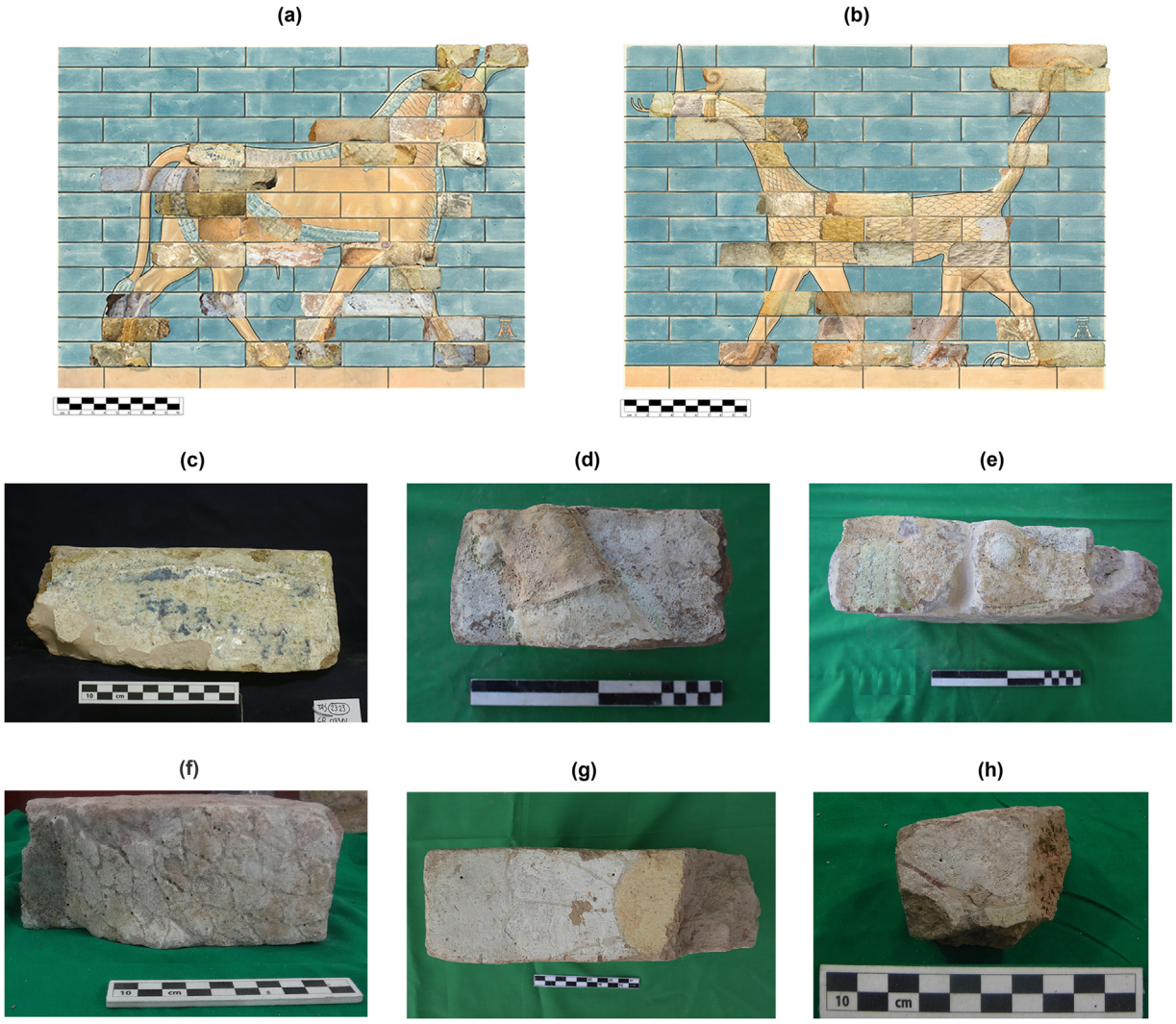

Fig. 1. Insertion of the fragments of decorated bricks from Tol-e Ajori in a reconstructed scheme of the Babylonian panel with **(a)** a bull motif in profile to the right and **(b)** a *mušḫuššu* motif in profile to the left. Drawing I. Arlotti, © Iranian-Italian Joint Archaeological Mission in Fars **(c-h)** Six decorated brick fragments from Tol-e Ajori and analysed by XRF and Vis-RS.

bricks of Tol-e Ajori, like those of the Ishtar Gate, show different parts of the bull (Fig. 1a,c,d) and the Mesopotamian snake dragon [6] (Fig. 1b,e,f) known as *mušḫuššu* [9]. These discoveries are in agreement with the results of the excavations, which show that the plan of the monumental gate of Tol-e Ajori repeats that of the inner section of the Ishtar Gate of Babylon [10], albeit on a larger scale and with significant modifications [1,2]. As regards the hues most of the Tol-e Ajori bricks are severely damaged: the glazes are generally decolourized and leached and, in many cases, crizzling and spalling phenomena are visible on the glazed surface [11].

The different elements represented on the brick panels (in relief or flat) – like those from the Ishtar Gate [12] – are outlined by a dividing line to separate them and to avoid the different glazes mixed before and during the firing in the kiln. The outlines on Tol-e Ajori bricks [6] are not in relief but sinking in the glazes (Fig. 1g,h). A similar line was used on the Achaemenid decorated bricks of Susa and the Persepolis Terrace, although in those cases the lines are clearly in relief and black/dark in colour [13,14].

The similarity between the figurative panels of the Tol-e Ajori monumental gate and the Ishtar Gate is not only in iconography, colour, proportions and size: each glazed brick from Tol-e Ajori that forms part of the figurative panels has been copied from the Babylonian panels down to the smallest detail. Moreover, archaeometric analyses showed that the bricks of the Tol-e Ajori gate were produced from local calcareous clays [15,16], and thus indicate that these 'Late Babylonian' style artefacts were produced in the heart of the Achaemenid empire [9,17].

2. Research aim

The glazed bricks used in the Tol-e Ajori monumental gate, recently discovered in Fars, Iran, are affected by intense deterioration processes due to the long burial. So, the first focus of this work was to define the original glaze hues of the unearthed bricks using non-invasive procedures. Moreover, a multi-analytical approach based on microscopic and spectroscopic analyses was used to characterize the Achaemenid polychrome glazed bricks and to compare them with the glazed bricks from significant sites in Iran and Iraq, such as the Ishtar Gate. In addition, the Co provenance was considered by comparing Tol-e Ajori data with the analytical results related to other Achaemenid blue glazes from Susa and Persepolis Terrace.

3. Material and methods

About 300 glazed bricks and brick fragments were first studied by a non-invasive Dino-Lite portable 5Mpx digital microscope (DM), and an Oxford Instruments X-Met 8000 energy dispersive X-ray fluorescence (ED-XRF) device equipped with a Rh target X-ray tube operating both at 8 kV and 50 μA (for low atomic weight elements) and 40 kV and 8 μA (for high atomic weight elements). A 90 s measurement time (¾ dedicated to the 8 kV condition, ¼ to the 40 kV one) was chosen to maximize the signal-to-noise ratio and Bruker Artax software was employed to elaborate spectra. Multivariate statistical analysis was applied to the elemental composition data by considering the net area of the L-alpha lines (only for Pb and Sb) and K-alpha lines of the selected elements, to identify any additional latent information other than the apparent colour of the glazes. Hierarchical Cluster Analysis (HCA) and Principal Component Analysis (PCA) elaborations were carried out by the statistical packages of Originlab v8.0.

Visible reflectance spectrometry analysis (Vis-RS) was performed on the glazed surface of about 30 bricks and brick fragments, using a handheld spectrophotometer Minolta CM-2600d equipped with an integrating sphere: spectral range 360–740 nm, 10 nm acquisition step, d/8 geometry, UV included, 3 mm diameter spot (reduced to 2 mm^2 when needed), measurement time 1 s, specular component included and excluded. Vis-RS allowed also colorimetric measurements.

In order to verify locally the elemental composition of a degraded glaze, with a chromatically inhomogeneous surface, micro-X-ray fluorescence (μ-XRF) elemental maps were acquired only in one greyish glazed brick fragment using a Bruker M4-Tornado μ-XRF spectrometer, Rh target, working at 50 kV, 600 μA and 20 mbar pressure with pixel size 25 μm and acquisition time of about 500 s.

Based on non-invasive data, 31 samples (Fig. S2) were selected for micro-invasive analysis as shown in Table S1. Twenty-one brick fragments were embedded in an epoxy resin and carefully polished after curing the resin with progressively finer paper to be made into polished cross-sections. A few samples were carefully ground to a final thickness (usually 30 μm) to be made into polished thin sections. Transmitted and reflected light observations on cross-sections and thin sections of glazed bricks were performed using an OLYMPUS BX51 polarized light microscope equipped with fixed oculars of 10x and objectives with different magnifications (5, 10, 20, 50 and 100x), directly connected to Olympus SC50 camera and Stream Basic software for images acquisition. A Philips Quanta FEI 200 scanning electron microscope (ESEM) equipped with an energy dispersive X-ray spectrometer (EDS) (model 6103, Link Analytical Oxford UK) was used for elemental analysis with an accelerating voltage variable between 20 and 30 kV, a lifetime of 40 s and a working distance of 30 mm. Twenty-one samples were examined in both high and low vacuum depending on the typology of the samples (thin/cross-section or micro fragment). The samples weren't coated with a conductive thin layer, which could limit their further investigation. Micro-Raman analysis (μ-Raman) was performed on 4 representative samples with a LabRam instrument from the Jobin Yvon-Horiba, equipped with a red 633 nm laser, a Peltier-cooled (−70 °C) CCD detector with 1024 × 256 pixels with a spectral resolution of 1 cm^{-1} and spatial resolution 1 μm. The scanning time varied from 5 to 20 s with the laser power of 5 mW and Olympus long working distance objectives with 50x and 100x were used.

4. Results

The original hues of the Tol-e Ajori glazes are often no longer present because they are deeply affected by decay. However, ED-XRF data, carried out on 300 discoloured glazed and unglazed bricks, both in situ and in the deposits, assisted by multivariate statistical techniques (PCA and HCA) allowed the identification of 4 main groups characterized by the presence of the typical chromophore elements that should have been responsible for the original hues (Figs. 2a and S3, Tab. S2). Three main groups are attributable to the blue, yellow and white glazes (see below in the text, also for the colour of the ellipses/sets), while the fourth group of data cannot be clearly defined because the surface of the bricks is too altered (the points under the light grey ellipse in the centre). Some unglazed relief bricks were also analysed by ED-XRF to verify if they could be originally glazed, revealing very high Ca content with lower amounts of Si, in association with Fe, Al and K, confirming a calcareous clay body [15,16] and the absence of chromophore element linked to glaze.

Vis-RS was carried out on 31 glazed fragments selected from the 3 different groups identified by HCA and PCA allowing to chromatically characterize the discolouration and the degradation phenomena and verifying the potential and limits of the technique [18,19].

PLM (Fig. S4a,b) and ESEM-EDS investigations (Tab. S1) confirmed a calcareous clay body and highlighted the presence of an interface, thinner than 100 μm, generally showing a high content of Si, Al and Na together with Mg, Fe, (P, K, Cl), and Ca, without chromophore components. Tol-e Ajori glazes are lime-alkali [20] and different colouring agents and opacifiers have been employed to obtain the different hues. The glaze's thickness ranges between 1.2 and 2.8 mm. Many undissolved crystals of quartz, pyroxene and dark particles are spread in the unaltered glazes (Fig. S4c). Bubbles, which are produced due to released gases in the vitrified glaze during the firing, were also visible. The voids percentage is very high (about 30%), with many gas bubbles of various diameters, ranging from 90 to 2800 μm, sometimes filled by secondary calcite. Degradation of glaze, opaque crusts and iridescent areas arranged as laminar or ring-shaped and in concentric "Liesegang" structures are visible in the glazes [21] due to dealkalization mechanisms, such as leaching and network dissolution [22] that altered the original hues (Fig. S4b-d).

4.1. Cobalt and copper-containing glazes

PCA biplot on the ED-XRF data preliminary classified and segregated by HCA treatment (clusterization by Ward method, tested for both City-Block, Euclidean and Squared Euclidian distance) identify a cluster of samples highly associated with Co and Cu (Fig. 2a, blue 95%-confidence-ellipse confined samples from HCA visible in Fig. S3), as the elements responsible for the blue colour, together with Fe, Zn, Ni and Mn as trace elements. The heterogeneity of the distribution of Co and Cu, as well as the effects of the alterations of the blue glazes, that occurred during the centuries, was also evident in the Vis-RS and colorimetric measurements on the same areas, showing the variability in colour.

Vis-RS allowed detecting, in the pale blue and grey-bluish glazes, the presence of a Co-based chromophore group, similar to that measured on Co-coloured glasses [23]. In these cases, in fact, Vis-RS spectra show absorption bands (Fig. 3a) at about 530, 590–600 and 640–650 nm (more pronounced in curves 1 and 5 of the figure, relating to darker areas), typical of Co^{2+} in tetrahedral symmetry. The presence of Cu can also modify the spectrum in Cu and Co-containing samples, hiding the typical spectrum due to the Co chromophore (Fig. 3b, solid lines).

Cu chromophore has a characteristic broad absorption band at about 800 nm due to the *d-d* transition, not completely exhibited in the selected range (Fig. 3c), while a broad reflectance maximum at about 500–600 nm is due to the combination of copper (II) [24] and the glass absorption. In some samples this reflectance

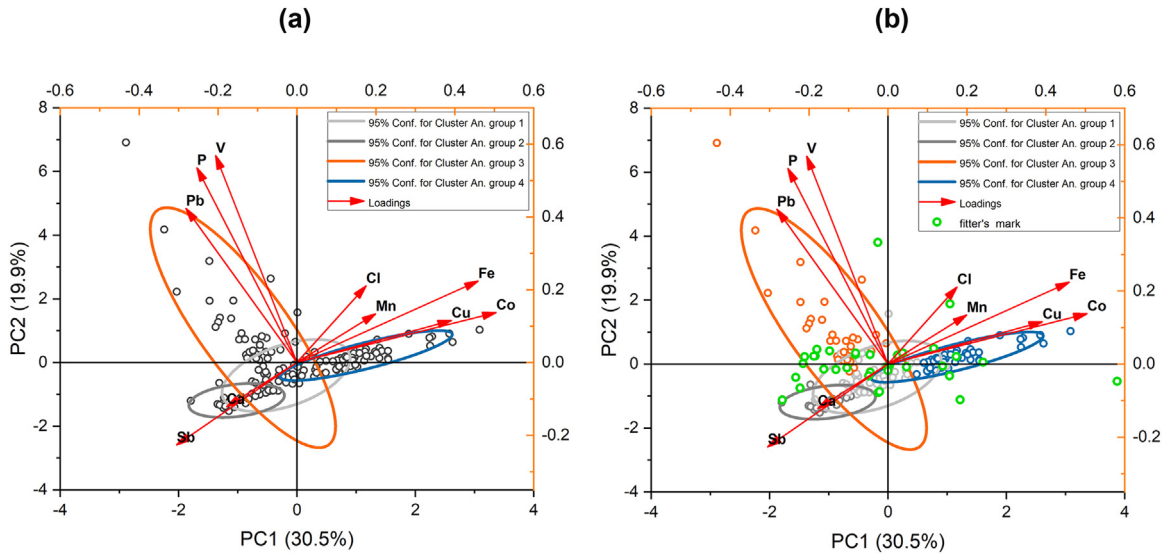

Fig. 2. **(a)** PCA biplots (loading and scored plots) based on ED-XRF spectra acquired on the glazed surfaces (excluding lateral and body samples) considering some significative elements; points are grouped and confined by the 95% confidence ellipses based on the clusterization derived from the Hierarchical Cluster Analysis (see Fig. S3); the colour of the ellipses has been attributed accordingly with the discussion; **(b)** Fitter marks composition -green circles- projected on the space of the 1st and 2nd PCs derived from the PCA (Fig. 2a) and HCA (Fig. S3).

peak shows a maximum around 600 nm, possibly influenced by the presence of iron oxides (as in Fig. 3b).

In the Vis-RS spectra of Co-based glazes, the loss of the reflectance peak in the blue region is rather pronounced in all the samples examined (curves 1, 14–15, Fig. 3a) due to discolouration phenomena, as demonstrated on Co-containing glasses like smalt blue pigments [25].

In some grey-bluish hues, Vis-RS allowed to identify a weak shoulder in the curves at 420–450 nm (Fig. 3b, curve 11) related to the effect of iron oxides (Fe^{3+} ions) with their typical c. 450 nm band. Generally, this signal can derive from the Fe oxides included in the glaze and also detected by EDS, while in the damaged glazes it is due to the clay bulk inside the lacunas (Fig. 3b, dotted curve 10).

EDS of bluish glaze confirmed the presence of both Fe-Co-rich particles and Cu filings. Rare crystal aggregates Sb-Ca based and very small in size (approximately 0.3–0.4 μm) were also found. In some grey-bluish glaze samples, the colouring agent is only Cu without Co and the opacifier agent is Ca antimonate.

μ-XRF mapping carried out on a grey-bluish sample (Fig. S5a,b) showed the heterogeneous distribution of Co and Cu in the grey-bluish glazes and, at a microscopical level, no significant relation between Cu and Co. Ca and P signals are related to the burial conditions while Si as a glaze component is uniformly distributed. In this sample, Pb is present at a trace level, while Fe and Mn cores are evident and generally unrelated. Co and Mn (and Cu to a lower extent) are usually more concentrated where black spots are present. In the bluish glazes (Fig. S6a), ESEM-EDS detected Cu and Co -coherently with the results of non-invasive analyses- sometimes with a variable amount of Fe (Fig. S6a,b).

In a few yellowish glazed bricks attributable to the curl of *mušḫuššu* and the bull's hoof (Fig. 1d,e), ED-XRF detected the unusual combination of Cu, Sb, Pb and Fe as confirmed by ESEM-EDS analysis. These decorative parts have been supposed to be greenish by the similarities with Babylonian glaze bricks (4,5,6). In these glazes, the reflectance peak lies between 560 and 580 nm (Fig. 3c, curves 49–51), shifted to longer wavelengths when the yellow hue is evident (curve 52) due to Sb and Pb, detected by XRF. As noted above, a weak shoulder in the Vis-RS curves at 420–450 nm is possibly due to Fe oxides.

It is interesting to mention that sometimes at the base of the glaze, very small (ca. 10 μm) particles rich in Ag, Pb, Cl and Sn were found (Fig. S6a,c) by ESEM-EDS. Similarly, a few particles rich in REE (La, Ce and Nd) and Ag were detected in a greenish glaze. Since Ag was only found in the blue glazes, it is most certainly linked with the colouring agent of these glazes; i.e. Co or Cu. No traces of Ag and REE were found in the portable ED-XRF and μ-XRF spectra of blue glazes, maybe due to the lower amount than the detection limit for these elements and to the fact that their characteristic X emissions are absorbed by the thick glassy matrix on the top since their presence is most probably restricted to the lower layer of the glazes (perhaps for a migration phenomenon due to gravity while firing), as found by ESEM-EDS.

In greenish glazes (Fig. 4a), very small Cu-filing were detected by ESEM-EDS (Fig. 4b,c). Large Fe-pellets were also detected showing a very rich border composed of glauconite elongated crystals (Fig. 4b,d). The Raman bands registered from the Fe-rich pellets (i.e. 174, 254, 563 and 694 cm^{-1}) which are consistent with the mineral glauconite ($(K,Na)(Fe^{3+},Al,Mg)_2(Si,Al)_4O_{10}(OH)_2$) [26] (Fig. 5a).

4.2. Lead antimonate opacified glazes

According to ED-XRF data, the group of glazes containing high amounts of Sb, Pb and Fe (orange 95% confidence ellipse confined points on the PCA biplot; Fig. 2a) suggested the presence of lead-based yellow glazes, associated with P, V, As and Cl other than Sb and Pb. Vis-RS spectra show a broad absorbence region below 480 nm (Fig. 3d) and a small shoulder at 450–460 nm related to the electronic transitions of Fe^{3+} ions, arranged in octahedral symmetry [27]. In addition, PCA confirmed that the composition of the fitters' marks was similar to that of the glazes (Fig. 2b).

PLM and ESEM-EDS analyses of the yellow glazes (Fig. S7a,b) confirmed the presence of Pb-Sb and Fe-based compounds. Regarding the lead antimonate crystallites (Fig. S7c), their shape and composition could be compared with iron-modified lead antimonate ($Pb_2Fe_{0:5}Sb_{1:5}O_{6:5}$), with the cubic crystal system (symmetry Fd-3 m (227)) [28,29]. Some of the yellow glazes and fitter's marks showed minor evidence of V in association with Pb, P and Cl (Fig. S8a,b).

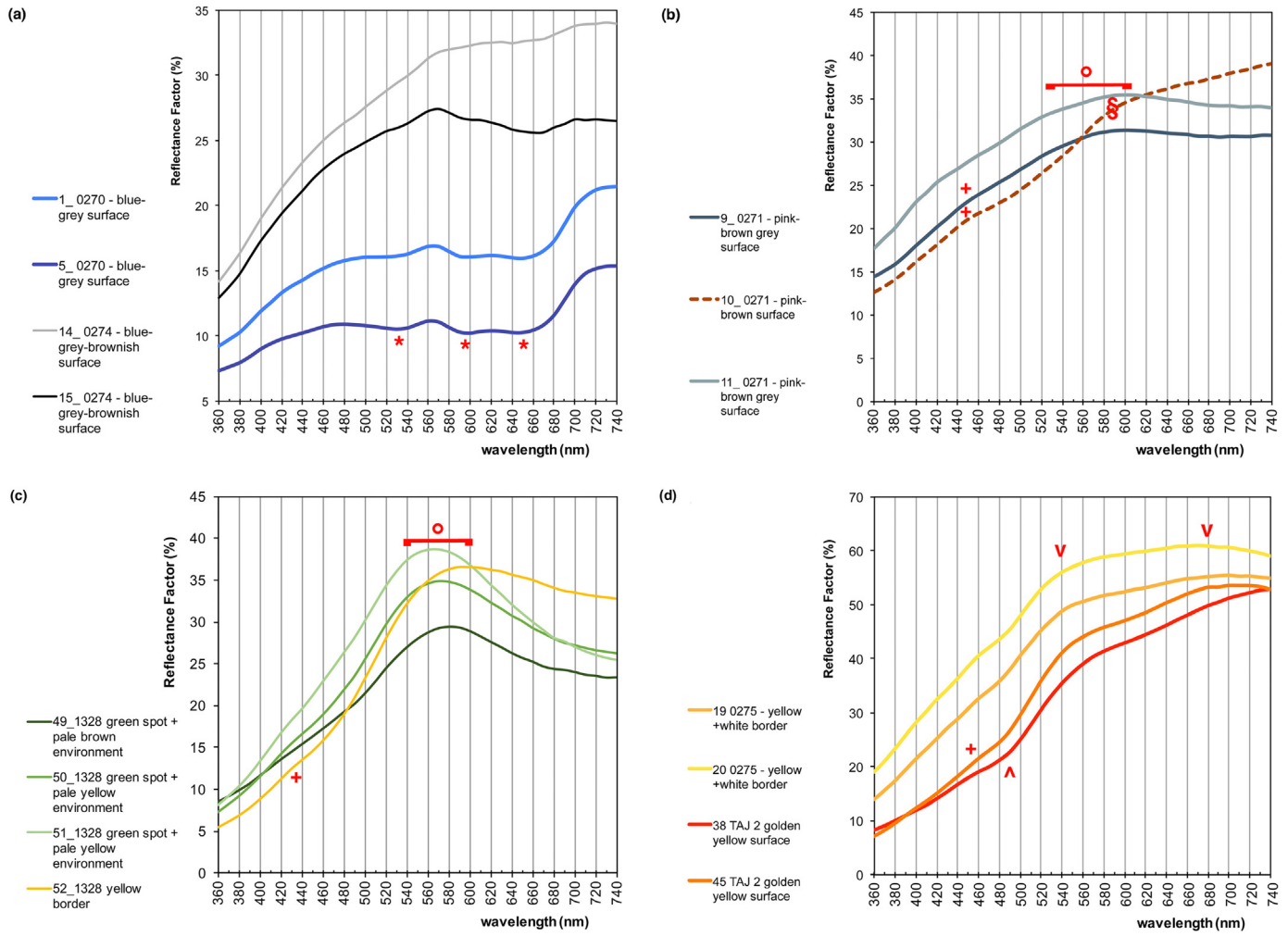

Fig. 3. **(a)** Vis-RS spectra of grey-bluish glazes containing Co) and Cu, where the first determines the final blue colour; **(b)** Vis-RS spectra of greyish glazes where Cu is prevalent (solid lines). The brown curve (dotted line) shows the effect of brown-pink earth deposits. The final colour of the surface is described as "pink-brown grey", due to these deposits; **(c)** Vis-RS spectra of greenish and yellow glazes containing Cu; **(d)** Vis-RS spectra of yellow or dark yellow glazes containing Pb and Sb. The elements Co, Cu, Pb and Sb were detected by ED-XRF and EDS analyses. The symbol * indicates the abs. sub-bands of Co^{2+} in tetrahedral symmetry; ° marks the broad peak due the combination of the glass and Cu^{2+} absorption; + the shoulder due to Fe^{3+} ions; § in the dotted line marks the shoulder typically related to goethite and to its c. 550 nm inflection point; ^ and v, respectively, the abs. edge and peaks linked to lead antimonate. Some shifts of reflectance peaks are evident, particularly for lighter surfaces, such as Fig. 3d.

In agreement with these observations, μ-Raman showed the significant occurrence of $Pb_2Sb_2O_7$ as the yellow opacifier in the glazes, with the Raman bands at 77, 96, 147, 206, 304, 339 and 517 cm^{-1} [30,31] (Fig. 5b). Also, μ-Raman revealed the occurrence of haematite (Fe_2O_3) in the glazes with the bands at 230, 249, 296, 415, 504, 618 and 667 cm^{-1} [32] (Fig. 5c) consistent with the major incorporation of Fe in the glaze. The presence of red haematite in the yellow glazes is the reason for their orangish colour.

4.3. Calcium and sodium antimonate opacified glazes

ED-XRF showed the major occurrence of Ca and Sb in the white samples (Fig. 2a, white 95% confidence ellipse confined dots and Fig. S3). The Raman bands at 241 and 675 cm^{-1} [32] showed the occurrence of calcium antimonate ($CaSb_2O_6$) incorporated as a white opacifier [33] (Fig. 5d). Apart from calcium antimonate, μ-Raman investigation on the white opacified glaze detected sodium antimonate ($NaSbO_3$, brizziite) with Raman bands at 160, 209, 236, 620 and 665 cm^{-1} [34] (Fig. 5e). The large contribution of two white opacifiers is an interesting feature of these glazes.

Digital microscope allowed to highlight that the outlines on Tol-e Ajori materials are sinking in the glazes (Fig. S9a,c). In a few cases, a Fe-rich red slip is present under the glaze (Fig. S9b). ESEM-EDS analysis confirmed the presence of calcium-antimonate in the white petals while the outline is distinguishable for the strong presence of Si (Fig. S9d), denoting the use of quartz powder. These white outlines are compositionally similar to the Neo-Assyrian ones [35].

5. Discussion

5.1. Antimonates as opacifiers

The occurrence of lead antimonate and calcium antimonate as yellow and white opacifiers in the vitreous materials of the Late Bronze Age and Iron Age in the Near East is well documented [36]. Lead antimonate, which has been reported to be the sole yellow opacifier used in the early Near Eastern vitreous materials, has been sometimes mixed with red haematite to produce orangish colour in the glaze [37,12]. Sodium antimonate has occasionally been identified in first-millennium glazed materials from north-

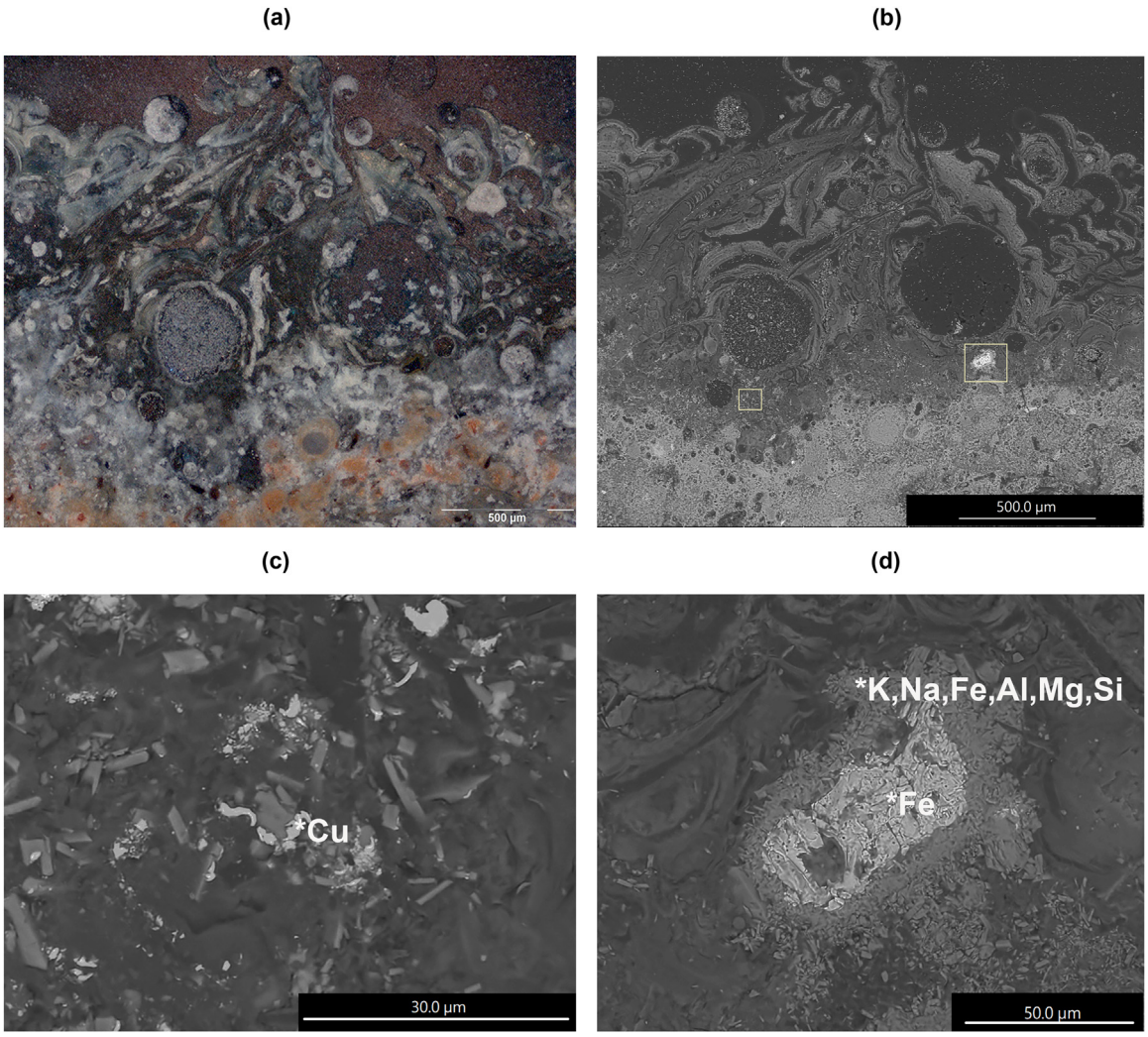

Fig. 4. Sample TAJ 2, cross-section: **(a)** PLM micrograph of the greenish glaze, reflected light; **(b)** BSE micrograph of the investigated areas; **(c)** BSE micrograph of Cu-filings; **(d)** BSE micrograph of Fe-pellet with a glauconite-rich border.

western Iran, as in the seventh century BC 'Mannaean' glazed bricks from Tepe Rabat [38] and in Achaemenid glazed bricks of Susa [39] and Persepolis Terrace [38].

Sodium antimonate is evidenced in the glazed bricks from Tol-e Ajori monumental gate but not in those from the Ishtar Gate [40,41] highlighting a major difference between them. However, there is no sufficient evidence to argue that sodium antimonate is absent in the glazes of Ishtar Gate, moreover, we are not able to discuss if the presence of sodium antimonate at Tol-e Ajori is a technological choice or accidental. If a deliberate choice, it has been suggested that sodium antimonate is formed in an alkali glaze when the Ca content of the glaze is consumed to precipitate Sb as calcium antimonate and there is still sufficient Sb content to be precipitated with the Na content of the glaze [42]. This can mean that: the amount of Ca of the glazes which incorporated sodium antimonate has not been high enough to precipitate the whole Sb content; or conversely, the Sb content has been high to satisfy both Ca and Na of the glazes at the expense of the formation of calcium and sodium antimonate. Therefore, the presence of $NaSbO_3$ in Tol-e Ajori glazed bricks should be an arbitrary accident resulting from high Sb or low Ca contents. Perhaps, a more in-depth isotopic study on the glazed materials from the Tol-e Ajori gate and a thorough comparison of the isotopic data with those available from the Ishtar Gate [43] will shed further light on the similarities/dissimilarities between the glaze technology from these very similar monuments.

5.2. Vanadium, phosphorus and chlorine

The presence of Pb, Cl and P in the yellow glazes is probably related to pyromorphite ($Pb_5(PO_4)_3Cl$) or lead hydroxyapatite. Pyromorphite is a secondary phase formed because of the retention of phosphate in the Pb-bearing glassy materials [44] due to the degradation phenomena [35]. Since the archaeological site of Tol-e Ajori is located in an agricultural field irrigated for many years, the corrosion of the glazes and incorporation of P and Cl available in that environment could support this claim. On the other hand, the presence of V in most of the P-Pb-bearing crystals, as well as the association of Pb with low amounts of V, Cl, As and P in Sb-deprived crystals, support the idea that the Pb-source for the glazes contained pyromorphite $Pb_5(PO_4)_3Cl$, vanadinite ($Pb_5(VO_4)_3Cl$) and mimetite ($Pb_5(AsO_4)_3Cl$). These minerals, belonging to the apatite group, occur in nature as a result of weathering of galena (PbS), the most common lead source used for glaze production in antiquity [45]. Interestingly, ancient Mesopotamian craftsmen have been familiar with a Pb-based substance called *kalgukku*, yellow and orangish in colour, used in glass and vitreous materials production in ancient Mesopotamia

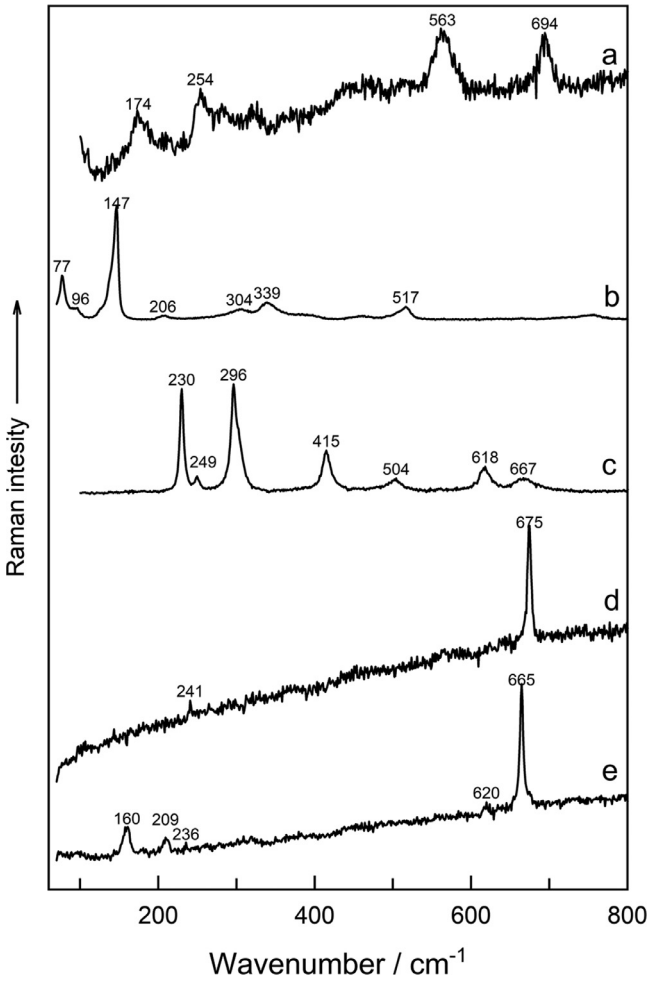

Fig. 5. Raman spectra of the glazes from Tol-e Ajori: **(a)** sample TAJ 2, glauconite; **(b)** sample TAJ 4, lead antimonate; **(c)** sample TAJ 4, haematite; **(d)** sample TAJ 3, calcium antimonate; **(e)** sample TAJ 3, sodium antimonate.

[45]. Thavapalan suggested [46] that this Pb-based material could be either minerals bindheimite ($Pb_2Sb_2O_6(O,OH)$), massicot (PbO) or wulfenite ($PbMoO_4$). However, there is no reason to rule out the connection of *kalgukku* with the aforementioned apatite group minerals. Thus, the possibility of the use of weathered galena with crusts of pyromorphite and vanadinite as the main source of Pb in the yellow glazes from Tol-e Ajori cannot be entirely excluded.

5.3. Source of Co

Blue was an important colour in ancient Iraq and Iran and at least from the Neo-Assyrian period, and it was used in the production of glazed bricks [47]. Since it was impossible to perform a quantitative study on the blue glazes of Tol-e Ajori due to their severe weathering, it is hard to establish a provenance for the Co source based only on the qualitative data.

The earliest Co sources used in early vitreous materials from Near East are reported from Dakhla Oasis [48] and the Western Oases in Egypt [49]. The Egyptian sources of Co were still in use in the glass industry of the first half of the first millennium BC at Nimrud [50], while the later first millennium AD vitreous materials of Nimrud show a different signature of Co source than those of Egyptian ones [51].

Similar to the Western Oases Egyptian source of Co, which shows Fe, Zn, Mn, Al and Ni as associated elements [48], the Co-coloured glazes from the 6th century BC Ishtar Gate are associated with Ni, Mn, Fe, Cu and Zn [43] suggesting that the Egyptian source of Co. Noteworthy, the bluish Co-coloured glazes from Tol-e Ajori demonstrate high Fe content, and minor trace amounts of Cu, Ni, Mn and Zn indicating the same Egyptian origin, and the fact that this source may have been still in use around the mid-first millennium BC.

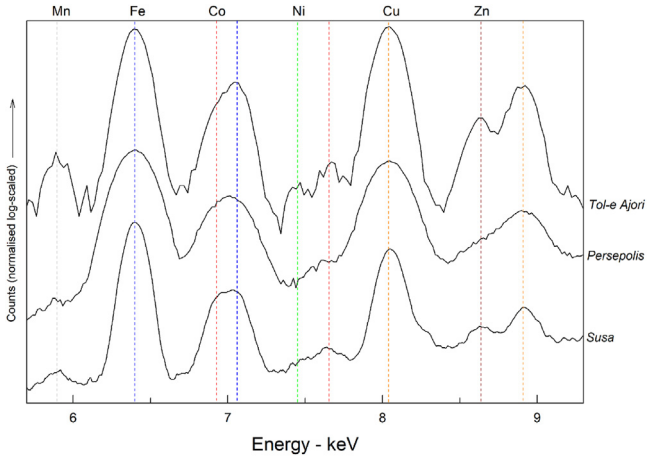

Fig. 6. A comparison among representative ED-XRF spectra acquired on Achaemenid blue glazes from Tol-e Ajori, Persepolis and Susa (the ED-XRF spectra from Persepolis Terrace and Susa are acquired from Holakooei et al. [37] and Holakooei [38] respectively).

Differently, the Achaemenid blue glazes at Susa [37] and Persepolis Terrace [38] differ for Mn, Ni and Zn contents from Tol-e Ajori and Ishtar gates (Fig. 6).

The change in the supply of Co-minerals is coherent with the dating proposed for the Tol-e Ajori monumental gate, which is thought to predate the buildings at Susa and the Persepolis Terrace.

Concerning Ag occurrence in a limited number of Tol-e Ajori blue glazes, there is no firm evidence for the occurrence of Ag in the ancient Near East Co-Cu blue-coloured glazes, while Dayton [52] reports that Co source of Mycenaeans blue glazes contains Ag. In any event, the mines of Co and Cu which contain Ag are nevertheless located almost exclusively in Europe and North America [51,53,54].

5.4. Glauconite as a degradation product

With regards to the occurrence of glauconite in the green glaze of the shard TAJ 2, it should be mentioned that since glauconite is transformed into other minerals phases in relatively low temperatures [55] and is not a stable phase in high firing temperatures that the glazed bricks have undergone (ca. 850 °C as shown by Amadori et al. [16]), it must have been formed as a result of the alteration of Fe-rich silicates originally used in the glazed bricks. Fe-rich minerals phases embedded in a siliceous matrix together with copper prills have been already reported to be the reason for the green colour in the eighth-century BC glazed materials from Nimrud [35]. Glauconite may have been formed due to the alteration of these Fe-rich aluminosilicates in the humid burial environment (the archaeological site of Tol-e Ajori is located in an agricultural field where irrigation is a routine practice).

6. Conclusions

From a methodological point of view, this research has shown that the mixed analytical approach, consisting of a first broad campaign of non-invasive XRF and Vis-RS analyses, possibly carried out

in situ, and a series of targeted in-depth analyses (ESEM-EDS, Raman, etc.) on selected micro-samples, represents an interesting operational protocol. Moreover, the reflectance measurements, often neglected for the study of ceramics, offer qualitative data useful for understanding the effective contribution of some elements, and related chromophore groups, to the final colour.

Thanks to the integrated investigations carried out on the glazed bricks of Tol-e Ajori monumental gate and the comparative research with the Ishtar Gate, it became possible to stress that white and orange-yellow glazes have been mainly used for the figurations, while blue glazes have been employed for the background and in the bull's details, exactly like in the Neo-Babylonian Ishtar Gate. In addition, some features of the animal body, like the *mušḫuššu* curl and bull hoof have been manufactured with greenish glazes.

The possible same source for Co as the colouring agent of blue glaze, the occurrence of lead antimonate and the use of clay bodies are the major technical similarities between the glaze technology of these two important monuments. The difference between them is in the presence of brizziite and calcium antimonate found as a white opacifier in the glazed bricks of Tol-e Ajori gate. Moreover, the use of a Fe-rich greenish glaze not evinced in the Ishtar Gate glazes could highlight another difference that occurred between these two monuments.

Despite comparative studies being limited by the amount of already published analyses on the glazes from various ancient Near East sites and future publications might bring new elements to this discussion, the results of the investigations underline that the production of the Tol-e Ajori bricks shows much more similarities with the earlier Neo-Assyrian and especially Neo-Babylonian technologies rather than the later Achaemenid glazed bricks at Susa and the Persepolis Terrace. A future isotopic study on the glazes from Tol-e Ajori could shed light on the provenance of the raw materials used to produce the decorated bricks.

Role of the funding source

This research did not receive any specific grant from the public, commercial, or not-for-profit funding agencies.

Data availability statement

As the data will be part of an ongoing study, the raw and processed data related to the glazed bricks cannot be shared at this time.

CRediT authorship contribution statement

Maria Letizia Amadori: Conceptualization, Methodology, Investigation, Data curation, Writing - original draft, Writing - review & editing, Funding acquisition. **Emad Matin:** Resources, Writing - original draft, Writing - review & editing, Supervision. **Gianluca Poldi:** Investigation, Data curation, Writing - review & editing. **Jgor Arduini:** Investigation, Data curation, Formal Analysis, Writing - review & editing. **Valeria Mengacci:** Investigation, Data and figures curation. **Alireza Askari Chaverdi:** Resources. **Pierfrancesco Callieri:** Resources. **Parviz Holakooei:** Investigation, Data curation, Writing - review & editing.

Acknowledgements

This research was carried out in the framework of the project 'From Palace to Town', thanks to the Iranian-Italian Joint Archaeological Mission in Fars of the Department of Cultural Heritage of the University of Bologna, the ISMEO, the Iranian Centre for Archaeological Research, the Persepolis World Heritage Foundation and the Shiraz University. Thanks are due to Sara Barcelli, Valentina Raspugli and Francesco Maria Mini for sample investigations and Laura Valentini for ESEM/EDS analysis collaboration. Thanks to Roald Tagle (Bruker Nano GmbH), Cristian Vailati and Mirko Gianesella (Bruker Optics, Milan) for the use of the μ-XRF TORNADO M6 spectrometer.

Supplementary materials

Supplementary material associated with this article can be found, in the online version, at doi:10.1016/j.culher.2023.01.005.

References

[1] A. Askari Chaverdi, P. Callieri, E. Matin, Tol-e Ajori, a monumental gate of the early Achaemenian period in the Persepolis area, in: The 2014 Excavation Season of the Iranian-Italian Project "From Palace to Town", with an Appendix by Gian Pietro Basello, a Fragment of Another Inscribed Glazed Brick from Tol-e Ajori, AMIT, 46, Deutsches Archaologisches Institut, Eurasian-Abteilung, Berlin, 2016, pp. 223–254.
[2] A. Askari Chaverdi, P. Callieri, E. Matin, The monumental gate at Tol-e Ajori, Persepolis (Fars): new archaeological data, Iran. Antiq. 52 (2017) 205–258.
[3] A. Askari Chaverdi, P. Callieri, Tol-e Ajori, Takht-e Jamshid: a sequence of imperial projects in the Persepolis area, East West 1 (1) (2020) 177–204.
[4] E. Matin, The decorated bricks, in: Tol-e Ajori: a monumental gate of the early Achaemenian period in the Persepolis Area. The 2014 excavation season of the Iranian-Italian project 'from Palace to Town', Archäologische Mitteilungen aus Iran und Turan 46 (2016) 239–246.
[5] E. Matin, New observations on the decorated bricks of Tol-e Ajori. In 'The Monumental Gate at Tol-e Ajori, Persepolis (Fars): new archaeological data', Iran. Antiq. 52 (2017) 232–240.
[6] E. Matin, in: E, Decorated Bricks from the Iranian-Italian Excavations at Tol-e Ajori (Fars), Department of Cultural Heritage, University of Bologna, Campus of Ravenna, 2014, pp. 108–125.
[7] M.S. Zeßin, Reading between the lines: fitters' marks in the Ancient Near East, in: A. Amrhein, C. Fitzgerald, E. Knott (Eds.), A Wonder to Behold: Craftsmanship and the Creation of Babylon's Ishtar Gate, ISAW, 2019, pp. 81–89.
[8] A. Fügert, H. Gries, The Reconstruction of the glazed brick facades from Ashur in the Vorderasiatisches Museum, Berlin (GlAssur Project), in: A. Fügert, H. Gries (Eds.), Glazed Brick Decoration in the Ancient Near East, Proceedings of a Workshop at the 11th International Congress of the Archaeology of the Ancient Near East (Munich) in April 2018, For the Vorderasiatischesche Museum – Staatliche Museen zu Berlin, Archaeopress Publishing LTD, Oxford, 2020, pp. 28–47.
[9] E. Matin, L'iconografia del *mušḫuššu* nel I millennio a.c, Parthica 23 (2021) 18–25 29.
[10] R. Koldewey,Das Ischtar-Tor in Babylon. Nach den Ausgrabungen durch die Deutsche Orient-Gesellschaft., J. C. Hinrichs, Leipzig, 1918, pp. 1–53.
[11] M.L. Amadori, et al., Micro-invasive investigations on bricks and glazed bricks from Tol-e Ajori, in: A. Askari Chaverdi, P. Callieri (Eds.), From Palace to Town. Report on the multidisciplinary project carried out by the Iranian-Italian Joint Archaeological Mission on the Persepolis Terrace (Fars, Iran), 2008-2013, 4, Science for Archaeology, Roma, 2017, pp. 59–110, doi:10.12977/from_palace_to_town_. a.
[12] F. Alloteau, et al., Microscopic-scale examination of the black and orange–yellow colours of architectural glazes from Aššur, Khorsabad and Babylon in Ancient Mesopotamia, Minerals 12 (3) (2022) 311, doi:10.3390/min12030311.
[13] A. Caubet, Achaemenid brick decoration, in: P.O. Harper, J. Aruz, F. Tallon (Eds.), The Royal City of Susa: Ancient Near Eastern Treasures in the Louvre, Metropolitan Museum of Art, New York, 1992, pp. 223–226.
[14] A. Caubet, in: Faïences et Matières Vitreuses de L'orient Ancient, Musée du Louvre, Paris, 2007, pp. 101–137.
[15] M.L. Amadori, et al., Scientific investigations on raw clay materials from Fars area, in: A. Askari Chaverdi, P. Callieri (Eds.), From Palace to Town. Report on the Multidisciplinary Project Carried Out by the Iranian-Italian Joint Archaeological Mission on the Persepolis Terrace (Fars, Iran), 2008-2013, 4, Science for Archaeology, Roma, 2017, pp. 6–19, doi:10.12977/from_palace_to_town_. b.
[16] M.L. Amadori, et al., Advances in Achaemenid Brick Manufacturing Technology: evidence from the monumental gate at Tol-e Ajori (Fars, Iran), Appl. Clay Sci. 152 (2018) 131–142, doi:10.1016/j.clay.2017.11.004.
[17] E. Matin, in: Early Achaemenian Architecture and Monumental Art in Fars and the Persian Gulf Region, Dipartimento di Beni Culturali, University of Bologna, Campus of Ravenna, 2018, pp. 174–183.
[18] A. Galli, G. Poldi, M. Martini, C. Montanari, E. Sibilia, Study of blue colour in ancient mosaic tesserae by means of luminescence and reflectance measurements, Appl. Phys. A: Mater. Sci. Process. 83 (2006) 675–679, doi:10.1007/s00339-006-3588-y.
[19] T. Pradell, J. Molera, Ceramic technology. How to characterise ceramic glazes, Archaeol. Anthropol. Sci. 12 (2020) 189, doi:10.1007/s12520-020-01136-9.
[20] Tite the technology of glazed Islamic ceramics using data collected by the late Alexander Kaczmarczyk, Archaeometry 53 (2011) 329–339, doi:10.1111/j.1475-4754.2010.00546.x.

[21] M. Maggetti, The introduction of the tin opacified glaze technique in Switzerland at the end of the 15th century CE – a SEM study of stove tiles from the canton Bern, J. Archaeol. Sci. Rep. 34 (2020) 102601 Part A, doi:10.1016/j.jasrep.2020.102601.
[22] N. Zacharias, et al., Archaeological glass corrosion studies: composition, environment and content, Sci. Cult. 6 (3) (2020) 53–67.
[23] M. Bacci, M. Picollo, Non-destructive spectroscopic detection of cobalt (II) in paintings and glass, Stud. Conserv. 41 (3) (1996) 136–144, doi:10.2307/1506528.
[24] A. Galli, et al., Thermoluminescence and visible reflectance spectroscopy applied to the study of blue-green mosaic silica-glass tesserae, Phys. Status Solidi C 4 (3) (2007) 950–953, doi:10.1002/pssc.200673863.
[25] G. Poldi, L'individuazione del blu di smalto sano e decolorato in dipinti mediante ED-XRF e spettrometria in riflettanza, in: A.T.I.V. Primo (Ed.), convegno interdisciplinare sul vetro nei beni culturali e nell'arte di ieri e di oggi, Associazione Tecnici Italiani del Vetro, Parma, 2009, pp. 11–21.
[26] F. Ospitali, et al., 'Green earths': vibrational and elemental characterization of glauconites, celadonites and historical pigments, J. Raman Spectrosc. 39 (2008) 1066–1073, doi:10.1002/jrs.1983.
[27] M. Elias, et al., The colour of ochres explained by their composition, Mater. Sci. Eng. B 127 (2006) 70–80, doi:10.1016/j.mseb.2005.09.061.
[28] C. Cascales, et al., The new pyrochlores $Pb_2(M_{0:5}Sb_{1:5})O_{6:5}$ (M = Al, Sc, Cr, Ga, Rh), Mater. Res. Bull. 20 (1985) 1359–1365.
[29] T.V. Yuryeva, et al., Microcrystals of antimony compounds in lead–potassium and lead glass and their effect on glass corrosion: a study of historical glass beads using electron microscopy, J. Mater. Sci. 53 (2018) 10692–10717, doi:10.1007/s10853-018-2332-2.
[30] R.J.H. Clark, et al., Synthesis, structural characterisation and Raman spectroscopy of the inorganic pigments lead tin yellow types I and II and lead antimonate yellow: their identification on medieval paintings and manuscripts, J. Chem. Soc., Dalton Trans. 16 (1995) 2577-2282.
[31] F. Rosi, et al., Raman scattering features of lead pyroantimonate compounds. Part I: XRD and Raman characterization of $Pb_2Sb_2O_7$ doped with tin and zinc, J. Raman Spectrosc. 40 (2009) 107–111, doi:10.1002/jrs.2699.
[32] M. Hanesch, Raman spectroscopy of iron oxides and (oxy)hydroxides at low laser power and possible applications in environmental magnetic studies, Geophys, J. Int. 177 (2009) 41–948, doi:10.1111/j.1365-246X.2009.04122.x.
[33] P. Ricciardi, et al., A non-invasive study of Roman age mosaic glass tesserae by means of Raman spectroscopy, J. Archaeol. Sci. 36 (2009) 2551–2559, doi:10.1016/j.jas.2009.07.008.
[34] R.L. Frost, S. Bahfenne, Raman spectroscopic study of the antimonate mineral brizziite $NaSbO_3$, Radiat. Effects Defects Solids: Incorporating Plasma Sci. Plasma Technol. 165 (3) (2010) 206–210, doi:10.1080/10420150903513046.
[35] P. Holakooei, et al., Glaze composition of the iron age glazed ceramics from Nimrud, Hasanlu and Borsippa preserved at the Metropolitan Museum of Art, J. Archaeol. Sci. Rep. 16 (2017) 224–232 b, doi:10.1016/j.jasrep.2017.09.031.
[36] P. Holakooei, Scientific research on the iron age glazes from Iran and Iraq: past and future, in: A. Fügert, H. Gries (Eds.), Ancient Near East, Proceedings of a Workshop at the11th International Congress of the Archaeology of the Ancient Near East (Munich) in April 2018, For the Vorderasiatisches Museum – Staatliche Museen zu Berlin, Archaeopress Publishing LTD, Oxford, 2020, pp. 16–27.
[37] P. Holakooei, A multi-spectroscopic approach to the characterization of early glaze opacifiers: studies on an Achaemenid glazed brick found at Susa, southwestern Iran (mid-first millennium BC), Spectrochim. Acta A Mol. Biomol. Spectrosc. 116 (2013) 49–56, doi:10.1016/j.saa.2013.07.002.
[38] P. Holakooei, et al., Early opacifiers in the glaze industry of the first millennium BC Persia: Persepolis and Tepe Rabat, Archaeometry 59 (2) (2017) 239–254 a, doi:10.1111/arcm.12255.
[39] M. Jung, A. Hauptmann, Report on the scientific examination of a glazed brick from Susa: colours, in: Persiens Antike Pracht – Band 2, Deutschen Bergbau–Museums Bochum, Buchum, 2004, pp. 390–392.
[40] S.C. Fitz, The coloured glazes of neo-Babylonian wall facings, Ceramic Forum Int.: Berichte der Deutsch Keramischen Gesellshaft 59 (1983) 179–185.
[41] F.R. Matson, Glazed bricks from Babylon: historical setting and microprobe analyses, in: W.D. Kingery (Ed.), Ceramics and Civilization II, Technology and Style, American Ceramic Society, Columbus, 1986, pp. 133–152.
[42] M.S. Tite, A.J. Shortland, Report on the scientific examination of a glazed brick from Susa: glazes, in: Persiens Antike Pracht – Band 2, Deutschen Bergbau–Museums, Bochum, 2004, pp. 388–390.
[43] A.S. Rodler, et al., Probing the provenance of archaeological glaze colorants: polychrome faunal reliefs of the Ishtar Gate and the Processional Way of Babylon, Archaeometry 61 (2019) 837–855, doi:10.1111/arcm.12455.
[44] I.C. Freestone, N.D. Meeks, A.P. Middleton, Retention of phosphate in buried ceramics: an electron microbeam approach, Archaeometry 27 (1985) 161–177, doi:10.1111/j.1475-4754.1985.tb00359.x.
[45] M.F. Keim, G. Markl, Weathering of galena: mineralogical processes, hydrogeochemical fluid path modelling, and estimation of the growth rate of pyromorphite, Am. Min. 100 (7) (2015) 1584–1594, doi:10.2138/am-2015-5183.
[46] S. Thavapalan, Stones from the mountain, stones from the kiln: colour in the glass texts from ancient Mesopotamia, in: S. Thavapalan, D.A. Warburton (Eds.), The Value of Colour: Material and Economic Aspects in the Ancient World, Edition Topoi, Topoi—Berlin Studies of the Ancient World 70, Berlin, 2019, pp. 177–200.
[47] W. Reade, I.C. Freestone, St. J., Innovation or continuity? Early first millennium BCE glass in the Near East: cobalt blue glasses from Assyrian Nimrud, in: H. Cool (Ed), Annales Du 16e Congrès de L'association Internationale Pour L'histoire Du Verre, London, 2005, pp. 23–27.
[48] A. Kaczmarczyk, The source of cobalt in ancient Egyptian pigments, in: J.S. Olin, M.J. Blackman (Eds.), Proceedings of the 24th International Archaeometry Symposium, Smithsonian Institution Press, Washington DC, 1986, pp. 369–376.
[49] A.J. Shortland, M.S. Tite, I. Ewart, Ancient exploitation and use of cobalt alums from the western oases of Egypt, Archaeometry 48 (2006) 153–168, doi:10.1111/j.1475-4754.2006.00248.x.
[50] J.E. Reade, A glazed brick panel from Nimrud, Iraq 25 (1963) 38–47.
[51] B. Gratuze, I. Pactat, N. Schibille, Changes in the signature of cobalt colorants in late antique and Early Islamic glass production, Minerals 8 (2018) 225, doi:10.3390/min8060225.
[52] J.E. Dayton, Geological evidence for the discovery of cobalt blue glass in Mycenaean times as a by-product of silver smelting in the Schneeberg area of the bohemian Erzgebirge, Revue d'Archéométrie, n°1, in: Actes du XXe symposium international d'archéométrie Paris 26-29 mars 1980 Volume III, 1981, pp. 57–61.
[53] S.A. Kissin, Five-element (Ni-Co-As-Ag-Bi) veins, Geosci. Canada 19 (1992) 113–124 https://journals.lib.unb.ca/index.php/GC/article/view/3768.
[54] P. Colomban, B. Kirmizi, G.S. Franci, Cobalt and associated impurities in blue (and green) glass, glaze and enamel: relationships between raw materials, processing, composition, phases and international trade, Minerals 11 (6) (2021) 633, doi:10.3390/min11060633.
[55] M.M. Haaland, et al., Heat-induced alteration of glauconitic minerals in the Middle Stone Age levels of Blombos Cave, South Africa: implications for evaluating site structure and burning events, J. Archaeol. Sci. 86 (2017) 81–100, doi:10.1016/j.jas.2017.06.008.